Drug Delivery

International Edition: DOI: 10.1002/anie.201606065
German Edition: DOI: 10.1002/ange.201606065

Nanoscale Biodegradable Organic–Inorganic Hybrids for Efficient Cell Penetration and Drug Delivery

*Sebastian Hörner[+], Sascha Knauer[+], Christina Uth[+], Marina Jöst, Volker Schmidts, Holm Frauendorf, Christina Marie Thiele, Olga Avrutina, and Harald Kolmar**

Abstract: *We report a comprehensive study on novel, highly efficient, and biodegradable hybrid molecular transporters. To this end, we designed a series of cell-penetrating, cube-octameric silsesquioxanes (COSS), and investigated cellular uptake by confocal microscopy and flow cytometry. A COSS with dense spatial arrangement of guanidinium groups displayed fast uptake kinetics and cell permeation at nanomolar concentrations in living HeLa cells. Efficient uptake was also observed in bacteria, yeasts, and archaea. The COSS-based carrier was significantly more potent than cell-penetrating peptides (CPPs) and displayed low toxicity. It efficiently delivered a covalently attached cytotoxic drug, doxorubicin, to living tumor cells. As the uptake of fluorescently labeled carrier remained in the presence of serum, the system could be considered particularly attractive for the in vivo delivery of therapeutics.*

Since Linus Pauling's groundbreaking publication in *Science*[1] in 1949, achievements in the rapidly advancing field of molecular medicine and related areas are very impressive. However, while today a vast arsenal of potent and selective drugs is available, an efficient strategy to deliver these therapeutic compounds inside the cell, in particular, in the cell nucleus, has become as important as the design and optimization of the pharmacophore itself. Considering that promising newly developed potential drug candidates, such as peptides and proteins, are water-soluble, a bottleneck in their application in living systems is the passage across the cellular membrane. As a consequence, drug delivery has emerged as one of the major fields in biomedical research. In 1994, the first cell-penetrating peptide (CPP) penetratin was described as a vehicle for cargo delivery into cells.[2] Since then, CPPs were thoroughly investigated and improved.[3] However, several issues associated with toxicity, stability, and efficacy of cellular uptake still require work. As the peptidic structure of CPPs intrinsically limits the scope of improvements, recent efforts are focused on nanoparticles or small non-peptidic molecular scaffolds.[4] These simple, uniform molecular architectures can be easily tailored, leading to cell-penetrating molecules with entirely new properties. In contrast to the macromolecular delivery systems, such as (bio)polymers, dendrimers, lipid-based or viral-like carriers, some of which are actually on the market or under clinical trials,[4c] the next-generation molecular transporters still require optimization.

General strategies towards the improvement of cellular uptake include the reduction of conformational freedom by backbone cyclization of cell-penetrating peptides or by the usage of scaffolds which induce spatial organization of the uptake-mediating functional groups.[3a,4d,5] Interestingly, the proximity of the charged groups to the backbone was found to influence the efficiency of cell uptake as well.[3c,d,5c,6]

Herein, we chose the cube-octameric silsesquioxane scaffold (COSS) as the starting point for the development of new-generation cell-penetrating compounds. COSS are highly ordered organic–inorganic hybrid molecules with a cage-like core of alternating silicon and oxygen atoms surrounded by eight pendant organic residues. Such an architecture with charged groups located at the flanking arms tethered to a compact (0.7 nm)[7] core ensures a compact, rigid, and symmetric construct. Generally, COSS are used in certain medical fields, for example, tissue engineering, or for the oligomerization of bioactive ligands, among them peptides and carbohydrates.[7,8] They are considered non-toxic and the hydrolytic degradation of the inorganic core under physiological conditions has been thoroughly investigated.[7]

COSS bearing seven ammonium groups were found to penetrate cells.[7,9] We have previously shown that these molecules enable the delivery of a functional peptidic cargo into living HeLa cells.[10] To improve this drug delivery system, we synthesized a series of COSS-based molecular transporters and investigated the uptake efficacy of a covalently attached cytotoxic drug.

Compounds **2**–**7** were synthesized following a two-step procedure (Scheme 1). Thus, inexpensive octaammonium COSS hydrochloride **1** was functionalized with a) guanidinium groups positively charged under physiological conditions or b) permanent positive charges installed by quaternary amines. Additionally, we investigated the influence of the flanking arm's length on cellular uptake. To visualize the constructs in cell assays, tetramethylrhodamine (TAMRA) was attached to a single corner of COSS **1** in a stoichiometri-

[*] S. Hörner,[+] S. Knauer,[+] C. Uth,[+] M. Jöst, Dr. O. Avrutina, Prof. Dr. H. Kolmar
Clemens-Schöpf-Institut für Organische Chemie und Biochemie
Technische Universität Darmstadt
Alarich-Weiss-Strasse 4, 64287 Darmstadt (Germany)
E-mail: kolmar@biochemie-tud.de
Dr. V. Schmidts, Prof. Dr. C. M. Thiele
Clemens-Schöpf-Institut für Organische Chemie und Biochemie
Technische Universität Darmstadt
Alarich-Weiss-Strasse 16, 64287 Darmstadt (Germany)
Dr. H. Frauendorf
Institut für Organische und Biomolekulare Chemie
Georg-August Universität Göttingen
Tammannstrasse 2, 37077 Göttingen (Germany)
[+] These authors contributed equally to this work.

Supporting information for this article can be found under: http://dx.doi.org/10.1002/anie.201606065.

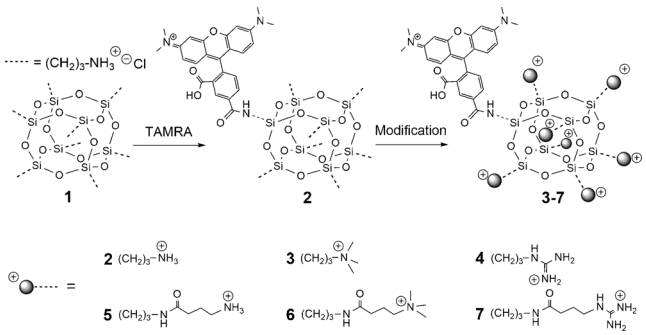

Scheme 1. Synthesis of fluorescently labeled cell-penetrating COSS derivatives **2**–**7** equipped with cationic functional groups separated from the core by spacers of different lengths. Counterions are excluded for clarity. Sequences of CPPs are shown in Supporting Information 5.2.

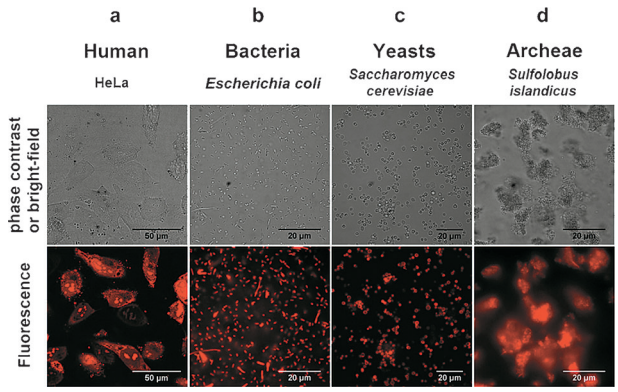

Figure 1. Cell uptake of TAMRA-GuCOSS (**4**). a) Live-cell laser scanning confocal microscopy imaging of HeLa cells incubated with **4** at 37 °C; b)–d) fluorescence microscopy imaging of cells incubated with **4**; b) Gram-negative bacterium (*E. coli*); c) yeast (*Saccharomyces cerevisiae*), both incubated at 37 °C; d) archaeon (*Sulfolobus islandicus*) incubated at 80 °C.

cally controlled reaction leading to TAMRA-aminoCOSS (**2**). Subsequently, the remaining seven amine functionalities of **2** were converted into the corresponding quaternary amines by N-methylation (TAMRA-quartCOSS **3**) or guanidinylation (TAMRA-GuCOSS **4**). Alternatively, for the introduction of a linker separating the siloxane core and the charged elements, 4-aminobutyric, 4-trimethylaminobutyric, or 4-guanidinobutyric acids were installed via amide coupling leading to, respectively, TAMRA-aminoCOSS-L (**5**), TAMRA-quartCOSS-L (**6**), and TAMRA-GuCOSS-L (**7**) (Scheme 1). To investigate toxicity of molecular transporters we synthesized amino-GuCOSS (**8**) lacking a fluorescent label (Supporting Information 5.2). Fluorescein-TAMRA-GuCOSS (**9**) was designed to assess biodegradation of the carriers (Figure 3 a). The integrity of the cage-like siloxane core was confirmed by NMR spectroscopy (compounds **2**–**7**; Supporting Information 5.3).

Fluorescently labeled derivatives **2**–**7** were investigated for their ability to penetrate living cells. To qualitatively estimate the uptake, we performed live-cell imaging using confocal laser scanning microscopy. Thus, HeLa cells were incubated with compounds **2**–**7** at a concentration of 20 µM in serum-free Dulbecco's modified eagle medium (DMEM) for 30 min. The cells were washed three times with phosphate buffered saline (PBS) and imaged in DMEM with fetal bovine serum (FBS). Compounds **2**–**4** bearing shorter linkers (Figure 1 a, Figure S1) demonstrated enhanced cellular uptake and prominent accumulation inside the nucleus, the nucleoli, and the cytoplasm, whereas an increase of the spacer's length led to reduced cellular uptake and primarily cytoplasmic localization (compounds **5**–**7**, Figure S1). In view of predominant accumulation in the nucleus, molecular transporters **2**–**4** are particularly attractive for the delivery of drugs addressing this cellular compartment.

As the guanidinylated carrier TAMRA-GuCOSS (**4**) exhibited the highest uptake in HeLa cells, its ability to penetrate cells from all three domains of life was further studied. The microscopic images obtained suggest that it is able to enter both eukaryotic and prokaryotic cells, among them yeast (*S. cerevisiae*) and mammalian cells (HeLa), as well as bacteria (*E. coli*) and archaea (*S. islandicus*, *S. tokodaii*, *Halobacterium salinarum*) (Figure 1 b–d, Figure S2). These observations are of particular interest in view of the exceptional membrane composition of archaea.[11] As guanidinylated COSS could be of interest for the delivery of antibiotics, we investigated its uptake in *E. coli* in detail (Figure S2c).

To quantify the cellular uptake in eukaryotic cells, we performed comprehensive flow-cytometric experiments with COSS derivatives **2**–**7** and TAMRA-labeled cell-penetrating peptides: TAT (**10**), penetratin (**11**), heptaarginine (**12**), and decaarginine (**13**).[12] We incubated HeLa cells with these compounds at a final concentration of 20 µM in serum-free DMEM at 37 °C up to 60 min. To remove surface-bound carrier molecules, cells were trypsinized (Supporting Information 5.1). Assays were performed in triplicate, the results were verified in three independent experiments (Figure S3a–g) with carrier **4** having shown the best cellular uptake. Indeed, the intensity of the fluorescence signal was found 155 times higher than that for the TAT peptide **10**. Interestingly, compound **4** carrying seven guanidinium groups displayed a 78-fold higher cellular uptake than heptaarginine (**12**; Figure 2 a). In agreement with our microscopy studies, shorter linkers correlated with enhanced fluorescence intensity (Figure S4). Similar results were obtained for HEK 293 and CHO cells (Figure S5a–c). This higher uptake of **4** can be attributed to its more compact arrangement, hence increased density of uptake-mediating functional groups. Indeed, cyclization of CPPs, leading to more constrained and rigid structures, is an efficient strategy to improve cellular uptake.[5c]

To evaluate whether the cellular uptake is energy-dependent, we compared the fluorescence intensity of HeLa cells incubated with **4** at 37 °C and at 4 °C (Figure 2 d). As the uptake was only negligibly decreased at 4 °C, an energy-independent mechanism was assumed. Time-resolved flow cytometry indicated fast uptake kinetics with a first shift of the population within an incubation time of 1 min at 37 °C (Figure S6). To determine the minimal internalization threshold, cells were incubated with **4** at different concentrations. Even at the lowest concentration (80 nM) a shift in fluores-

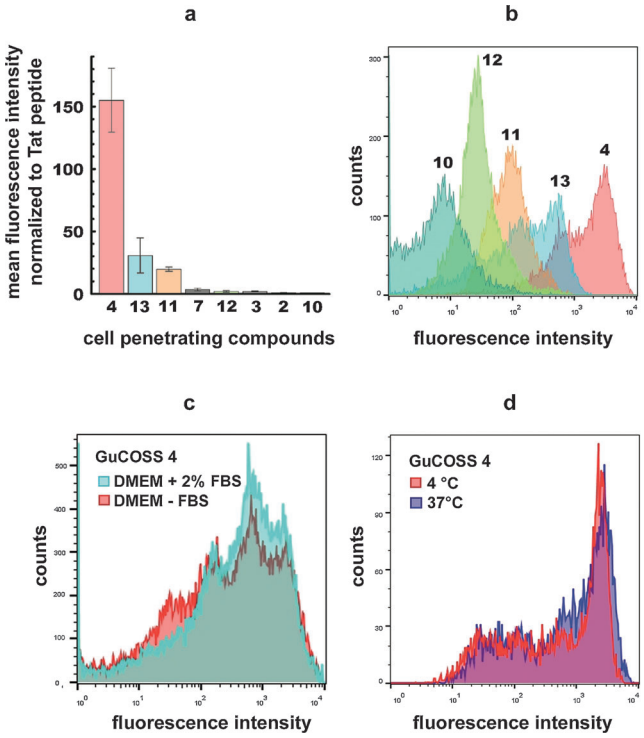

Figure 2. Flow-cytometric experiments using HeLa cells. a) mean fluorescence intensity of selected COSS derivatives and cell-penetrating peptides. b) representative histogram of TAMRA-GuCOSS (**4**) and cell-penetrating peptides (petrol-green: TAT (**10**); yellow-green: heptaarginine (**12**); orange: penetratin (**11**), light blue: decaarginine (**13**); red: TAMRA-GuCOSS (**4**). c) HeLa cells incubated with **4** in the presence and the absence of 2% FBS in DMEM. d) Cellular uptake of **4** in HeLa cells incubated in serum-free DMEM for 10 min with 20 μM **4** at 37 °C or 4 °C.

cence intensity was observed and 1 μM **4** was needed to reach full shift of the population after an incubation time of 10 min at 37 °C (Figure S7). In contrast to cell-penetrating peptides, no minimal internalization threshold within the investigated concentrations was observed.[13] As recent studies suggest that both the silsesquioxane core and guanidine groups promote clustering,[7,14] it could be supposed that high local concentration of **4** (as a result of its assembly on the cell surface) ensures cell penetration even at low concentrations. Our observations point to an energy-independent direct cell translocation, in accordance with the uptake mechanism of other polyguanidines.[13]

The uptake of cell-penetrating peptides is generally retarded in serum-containing media.[15] Impaired CPP-mediated permeation efficacy has been reported for polyarginines both in serum-containing media and in in vivo experiments, presumably owing to their aggregation with serum proteins. Therefore, we imaged **4** in the presence of 10% FBS in DMEM (Figure S8) and found that 40% of the mean fluorescence intensity was retained, compared to that for serum-free media.[3c,15a,16] This tolerance of serum proteins, combined with fast and effective cellular uptake, makes **4** a promising carrier for in vivo applications.

Since many cell-penetrating compounds were found to be toxic above a certain concentration, we investigated the toxicity of amino-GuCOSS (**8**) lacking a fluorescent label (Supporting Information 5.2) in HeLa cells using an XTT cell viability assay. Thereby the LC_{50} was determined to be 84 μM (Figure 3e), which is comparable to that of polyarginines (76 μM), TAT (86.6% viability at 50 μM), and penetratin (88.2% at 50 μM).[17] This low toxicity may be caused by biodegradation of the inorganic core under physiological conditions. Indeed, the pH-dependent degradation of polyhedral silsesquioxanes resulting in primary siloxanes is well established.[7]

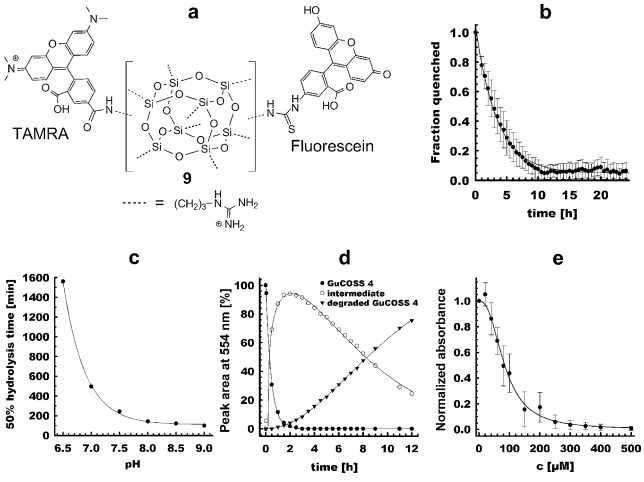

Figure 3. GuCOSS degradation studies. a) Guanidinylated COSS construct bearing the two fluorophores, fluorescein and TAMRA (Fluorescein-TAMRA-GuCOSS (**9**)). b) Decrease of the quenched fraction of fluorescein in the in vitro degradation studies in living HeLa cells. c) 50% hydrolysis of TAMRA-GuCOSS (**4**) as a function of the pH in PBS. d) Kinetics of the degradation of **4** at pH 7.0 in PBS analyzed by HPLC. e) XTT assay of the in vitro toxicity of guanidinylated COSS (**8**) bearing no fluorescent label.

For characterization of pH-dependent degradation of **4**, we monitored decomposition of the inorganic core by RP-HPLC. To that end, **4** was incubated in PBS at pH 6.5–9.0 (37 °C) and time-resolved HPLC traces were recorded within 12 h at 554 nm (absorption maximum of TAMRA). Hydrolysis intermediates and the degradation products were quantified by determination of the peak areas. Although hydroxyl-bearing intermediates were eluted earlier from the column, the completely hydrolyzed TAMRA-decorated siloxanes had longer retention times. Typical HPLC traces at pH 7.0 are shown at Figure S9, and respective half-life values at pH 6.5–9.0 in Figure 3c. Thereby, the $t_{1/2}$ at pH 7.4 (PBS) was determined to be 252 min. The degradation at neutral pH is shown in Figure 3d.

To assess the biodegradation of the GuCOSS-based carriers, we synthesized derivative **9** carrying two fluorescent markers, fluorescein and TAMRA (Figure 3a). As both dyes are attached to the same siloxane core in spatial proximity, the fluorescence of fluorescein is quenched upon Förster resonance energy transfer (FRET; Figure S10). As the inorganic core loses its integrity during breakdown, either fluorescein or TAMRA separates from the siloxane cage, and the fluorescence of fluorescein is restored. Along with excitation at

488 nm the increase of the emission at 520 nm was used to quantify the fraction of partially disassembled carriers. Based on the fluorescence recovery of fluorescein, a half-life of 186 min was found in human serum, indicating sufficient stability for in vivo applications (Figure S11). As HPLC analysis allowed the erosion process to be monitored up to the final degradation products, the half-life determined using this approach was significantly longer (252 min at pH 7.4). In former studies, the half-life of cell-penetrating peptides in the presence of serum was found to be in the range of minutes (e.g. $t_{1/2} = 5$ min for penetratin).[18] This fast decay is most likely caused by proteolysis. It is clear that the hybrid GuCOSS construct does not serve as a substrate for proteolytic enzymes. The enhanced half-life of derivative **9** in serum is an additional indication that the degradation of the COSS core is predominantly pH dependent.

To better understand how the degradation proceeds in living cells, we monitored the recovery of fluorescein fluorescence by live-cell confocal laser scanning microscopy upon internalization of construct **9** in HeLa cells (Figure 3b, Figure S12). The fluorescent markers were disconnected in half of the starting material within 149 min, and complete disassembly (reappearance of fluorescence) occurred in 11 h. The half-lives obtained in these experiments are on the same order of magnitude as those observed upon incubation in human serum ($t_{1/2} = 186$ min).

Applicability of GuCOSS as a molecular transporter was examined upon cellular delivery of a cytotoxic cargo doxorubicin (DOX, **14**)—a widely applied antitumor drug.[19] Being able to intercalate DNA, this agent induces apoptosis in cancer cells by activating the intrinsic death pathway.[20] Therefore, it is clear that the therapeutic effect of DOX could be exerted only if the drug gains access to the cell nucleus. However, because only passive diffusion ensures its penetration into tumor tissues, the efficiency of DOX is strongly compromised, which represents the major limitation of this highly potent compound.[21] In a model construct, we connected the GuCOSS delivery module to a DOX functional cargo via a disulfide yielding the conjugate **15** (Supporting Information 5.2). This bond is rapidly reduced in the reductive environment of cytosol, enabling drug release inside the cell.[22]

Cellular delivery was studied in HeLa cells. First, an incubation time-dependent cell assay with the free antibiotic was performed (Supporting Information 4.0, 5.1). Because of the slow uptake of free doxorubicin, the number of cancer cells killed correlated with the duration of incubation (Figure S13). The conjugate **15** as well as the controls (free doxorubicin (**14**) and untreated cells) were incubated at the same concentrations for 1 h (Supporting Information 3.0). Then the cells were washed with DMEM, and after 18 h an MTT assay was performed (Figure 4). The results clearly show that the hybrid construct **15** had an enhanced cytotoxic effect compared to the free drug **14**.

Although it is one of the cornerstones of cancer therapy, free doxorubicin causes irreversible cardiac damage.[23] Whereas its liposomal formulation[24] mitigates the toxic side effects,[23] the potency is unaltered compared to the conventional drug.[25] While the recently reported formulation

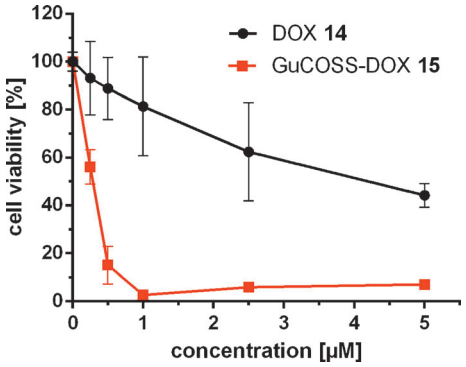

Figure 4. Cell viability assay (MTT) of free doxorubicin (DOX, **14**) and the doxorubicin-GuCOSS conjugate (**15**). Error bars indicate standard deviations from three independent measurements.

based on liposomal coencapsulation of DOX with Listeriolysin O enables enhancement of nuclear targeting in certain carcinoma cell lines, it is supposed to be highly immunogenic.[26] Therefore, we believe that our delivery platform combining highly efficient cell penetration with small size, low toxicity, and biodegradability might provide clear benefits. Nevertheless, further validation by animal studies is required, which particularly addresses cardiotoxic effects in comparison to liposomal doxorubicin formulations. It may also be interesting to investigate whether the cellular uptake of other cytotoxins with particularly low cell-penetrating efficacy, such as for example, hygromycin,[27] can be enhanced upon COSS conjugation.

To summarize, we developed new-generation hybrid cell-penetrating compounds based on the cube-octameric silsesquioxane scaffold. Thus, the guanidinylated fluorescent COSS derivative was found to efficiently penetrate cells from all three domains of life with a 155-fold enhanced, compared to the cell-penetrating peptide TAT, cellular uptake in HeLa cells. The carrier has fast uptake kinetics and penetrates cells at double-digit nanomolar concentrations. It has low toxicity and decomposes under physiological conditions within 11 h. This novel molecular transporter retains its activity in the presence of serum, which makes it a promising candidate for in vivo delivery of drugs. Taking into consideration that these organic–inorganic hybrids are very small and compact, no or weak immune response could be assumed. We believe that our delivery platform may enrich the toolbox of low-toxic and highly efficient molecular systems needed for the development of future-oriented therapeutics.

Acknowledgements

We thank Dr. Anna-Lena Krause (Nationales Centrum für Tumorerkrankungen, DKFZ, Heidelberg, Germany) for assistance during flow cytometry interpretation, Thomas Pirzer for providing HeLa cells, and PD Dr. Arnulf Kletzin (Fachbereich Biologie, Technische Universität Darmstadt) for providing *sulfobacter* and *archaea*.

Keywords: cell penetration · cell-penetrating compound · COSS · drug delivery · silsesquioxanes

[1] L. Pauling, H. A. Itano, S. J. Singer, I. C. Wells, *Science* **1949**, *110*, 543 – 548.

[2] D. Derossi, M. H. Joliot, G. Chassaing, M. Prochiantz, *J. Biol. Chem.* **1994**, *269*, 10444 – 10450.

[3] a) A. Ho, S. R. Schwarze, S. J. Mermelstein, G. Waksman, S. F. Dowdy, *Cancer Res.* **2001**, *61*, 474 – 477; b) A. Nasrolahi Shirazi, R. Tiwari, B. S. Chhikara, D. Mandal, K. Parang, *Mol. Pharm.* **2013**, *10*, 488 – 499; c) P. A. Wender, D. J. Mitchell, K. Pattabiraman, E. T. Pelkey, L. Steinman, J. B. Rothbard, *Proc. Natl. Acad. Sci. USA* **2000**, *97*, 13003 – 13008; d) P. A. Wender, J. B. Rothbard, T. C. Jessop, E. L. Kreider, B. L. Wylie, *J. Am. Chem. Soc.* **2002**, *124*, 13382 – 13383.

[4] a) V. Bagnacani, V. Franceschi, M. Bassi, M. Lomazzi, G. Donofrio, F. Sansone, A. Casnati, R. Ungaro, *Nat. Commun.* **2013**, *4*, 1721; b) S. Bersani, S. Salmaso, F. Mastrotto, E. Ravazzolo, A. Semenzato, P. Caliceti, *Bioconjugate Chem.* **2012**, *23*, 1415 – 1425; c) Z. G. Chen, *Trends Mol. Med.* **2010**, *16*, 594 – 602; d) N. W. Luedtke, P. Carmichael, Y. Tor, *J. Am. Chem. Soc.* **2003**, *125*, 12374 – 12375; e) M. Okuyama, H. Laman, S. R. Kingsbury, C. Visintin, E. Leo, K. L. Eward, K. Stoeber, C. Boshoff, G. H. Williams, D. L. Selwood, *Nat. Methods* **2007**, *4*, 153 – 159; f) J. Valero, M. Van Gool, R. Perez-Fernandez, P. Castreno, J. Sanchez-Quesada, P. Prados, J. de Mendoza, *Org. Biomol. Chem.* **2012**, *10*, 5417 – 5430.

[5] a) Y. A. Fillon, J. P. Anderson, j. Chmielewski, *J. Am. Chem. Soc.* **2005**, *127*, 11798 – 11803; b) N. P. Gabrielson, H. Lu, L. Yin, D. Li, F. Wang, J. Cheng, *Angew. Chem. Int. Ed.* **2012**, *51*, 1143 – 1147; *Angew. Chem.* **2012**, *124*, 1169 – 1173; c) G. Lättig-Tünnemann, M. Prinz, D. Hoffmann, J. Behlke, C. Palm-Apergi, I. Morano, H. D. Herce, M. C. Cardoso, *Nat. Commun.* **2011**, *2*, 453; d) D. Mandal, A. Nasrolahi Shirazi, K. Parang, *Angew. Chem. Int. Ed.* **2011**, *50*, 9633 – 9637; *Angew. Chem.* **2011**, *123*, 9807 – 9811; e) A. Nasrolahi Shirazi, R. K. Tiwari, D. Oh, B. Sullivan, K. McCaffrey, D. Mandal, K. Parang, *Mol. Pharm.* **2013**, *10*, 3137 – 3151; f) H. Tang, L. Yin, K. H. Kim, J. Cheng, *Chem. Sci.* **2013**, *4*, 3839.

[6] K. K. Maiti, W. S. Lee, T. Takeuchi, C. Watkins, M. Fretz, D. C. Kim, S. Futaki, A. Jones, K. T. Kim, S. K. Chung, *Angew. Chem. Int. Ed.* **2007**, *46*, 5880 – 5884; *Angew. Chem.* **2007**, *119*, 5984 – 5988.

[7] S. Fabritz, S. Hörner, O. Avrutina, H. Kolmar, *Org. Biomol. Chem.* **2013**, *11*, 2224 – 2236.

[8] a) S. Fabritz, S. Hörner, D. Konning, M. Empting, M. Reinwarth, C. Dietz, B. Glotzbach, H. Frauendorf, H. Kolmar, O. Avrutina, *Org. Biomol. Chem.* **2012**, *10*, 6287 – 6293; b) D. Heyl, E. Rikowski, R. C. Hoffmann, J. J. Schneider, W. D. Fessner, *Chem. Eur. J.* **2010**, *16*, 5544 – 5548.

[9] C. McCusker, J. B. Carroll, V. M. Rotello, *Chem. Commun.* **2005**, 996 – 998.

[10] S. Hörner, S. Fabritz, H. D. Herce, O. Avrutina, C. Dietz, R. W. Stark, M. C. Cardoso, H. Kolmar, *Org. Biomol. Chem.* **2013**, *11*, 2258 – 2265.

[11] M. De Rosa, A. Gambacorta, A. Gliozzi, *Microbiol. Rev.* **1986**, *50*, 70 – 80.

[12] a) D. Derossi, S. Calvet, A. Trembleau, A. Brunissen, G. Chassaing, A. Prochiantz, *J. Biol. Chem.* **1996**, *271*, 18188 – 18193; b) S. Futaki, T. Suzuki, W. Ohashi, T. Yagami, S. Tanaka, K. Ueda, Y. Sugiura, *J. Biol. Chem.* **2001**, *276*, 5836 – 5840; c) E. Vivès, P. Brodin, B. Lebleu, *J. Biol. Chem.* **1997**, *272*, 16010 – 16017.

[13] F. Duchardt, M. Fotin-Mleczek, H. Schwarz, R. Fischer, R. Brock, *Traffic* **2007**, *8*, 848 – 866.

[14] M. Vazdar, E. Wernersson, M. Khabiri, L. Cwiklik, P. Jurkiewicz, M. Hof, E. Mann, S. Kolusheva, R. Jelinek, P. Jungwirth, *J. Phys. Chem. B* **2013**, *117*, 11530 – 11540.

[15] a) M. Kosuge, T. Takeuchi, I. Nakase, A. T. Jones, S. Futaki, *Bioconjugate Chem.* **2008**, *19*, 656 – 664; b) I. Nakase, Y. Konishi, M. Ueda, H. Saji, S. Futaki, *J. Controlled Release* **2012**, *159*, 181 – 188; c) K. Park, *J. Controlled Release* **2012**, *159*, 153.

[16] A. F. Saleh, A. Arzumanov, R. Abes, D. Owen, B. Lebleu, M. J. Gait, *Bioconjugate Chem.* **2010**, *21*, 1902 – 1911.

[17] S. W. Jones, R. Christison, K. Bundell, C. J. Voyce, S. M. Brockbank, P. Newham, M. A. Lindsay, *Br. J. Pharmacol.* **2005**, *145*, 1093 – 1102.

[18] M. Hällbrink, J. Oehlke, G. Papsdorf, M. Bienert, *Biochim. Biophys. Acta Biomembr.* **2004**, *1667*, 222 – 228.

[19] A. M. Meredith, C. R. Dass, *J. Pharm. Pharmacol.* **2016**, *68*, 729.

[20] a) Y. Sun, X. Yan, T. Yuan, J. Liang, Y. Fan, Z. Gu, X. Zhang, *Biomaterials* **2010**, *31*, 7124 – 7131; b) S. Wesselborg, I. H. Engels, E. Rossmann, M. Los, K. Schulze-Osthoff, *Blood* **1999**, *9*, 3053 – 3063.

[21] A. I. Minchinton, I. F. Tannock, *Nat. Rev. Cancer* **2006**, *6*, 583 – 592.

[22] G. Saito, J. A. swanson, K. D. Lee, *Adv. Drug Delivery Rev.* **2003**, *55*, 199 – 215.

[23] T. Safra, *Oncologist* **2003**, *8*, 17 – 24.

[24] A. L. B. Seynhaeve, B. M. Dicheva, S. Hoving, G. A. Koning, T. L. M. ten Hagen, *J. Controlled Release* **2013**, *172*, 330 – 340.

[25] a) L. Harris, G. Batist, R. Belt, D. Rovira, R. Navari, N. Azarnia, K. Welles, E. Winer, T. D.-S. Grp, *Cancer* **2002**, *94*, 25 – 36; b) E. Rivera, *Oncologist* **2003**, *8*, 3 – 9.

[26] a) J. A. Carrero, H. Vivanco-Cid, E. R. Unanue, *Plos One* **2012**, *7*, e32310; b) Z. F. Walls, H. Gong, R. J. Wilson, *Mol. Pharm.* **2016**, *13*, 1185 – 1190.

[27] J. C. Lacal, L. Carrasco, *Antimicrob. Agents Chemother.* **1983**, *24*, 273 – 275.

Received: June 22, 2016
Revised: September 27, 2016
Published online: ■■ ■■, ■■■■

Communications

Drug Delivery

S. Hörner, S. Knauer, C. Uth, M. Jöst, V. Schmidts, H. Frauendorf, C. M. Thiele, O. Avrutina, H. Kolmar* ____ ▮▮▮▮–▮▮▮▮

Nanoscale Biodegradable Organic–Inorganic Hybrids for Efficient Cell Penetration and Drug Delivery

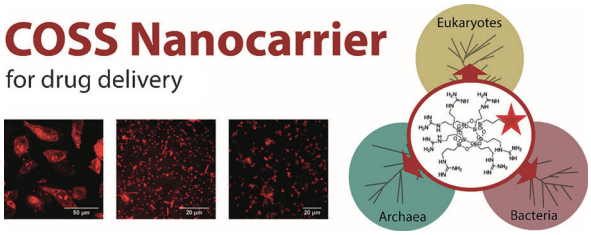

COSS and effect: New-generation molecular transporters are based on cell-penetrating cube-octameric silsesquioxanes (COSS). These nanoscale hybrid carriers are biodegradable, low-toxic, and show efficient uptake in living cells of all three domains of life.